RESEARCH ARTICLE

Design and Development of Nanostructured Co Delivery of Artemisinin and Chrysin for Targeting hTERT Gene Expression in Breast Cancer Cell Line: Possible Clinical Application in Cancer Treatment

Leila Khoshravan Azar[1], Mehdi Dadashpour[2,3]*, Mehrdad Hashemi[1], Nosratollah Zarghami[4,5]*

Abstract

Background: Breast cancer is one of the most significant causes of female cancer death worldwide. To explore the possibility of a novel chemo-preventive strategy for improving breast cancer treatment, the anticancer effects of two natural compounds, Artemisinin (Art) and Chrysin (Chr), against T47D breast cancer cells were investigated. **Methods:** For this purpose, Art and Chr were co-encapsulated in PEGylated PLGA nanoparticles (NPs) and the synthesized NPs were characterized by FE-SEM, FTIR, and DLS and then, MTT assay was used to assess and compare the cytotoxicity of various concentrations of the chemotheruptic molecules in pure and nanoformulated forms as well as in alone and combination state after 48 h exposure time. Drug release study was performed using the dialysis method. Also, the mRNA levels of *hTERT* genes expression were studied by quantitative real-time PCR. **Results:** The results showed that pure and formulations drugs exhibited dose-dependent cytotoxicity against T47D cells and especially, Art/Chr–PLGA/PEG NPs had a more synergistic anti-proliferative effect and significantly arrested the growth of cancer cells than the other groups. Moreover, Real-time PCR results revealed that Art, Chr and combination of Art–Chr in pure and encapsulated forms inhibited *hTERT* gene expression. **Conclusions:** It was found that Art/Chr–PLGA/PEG NPs relative to pure combination could further decline hTERT expression in all concentrations. Our study demonstrated that Art/Chr-PLGA/PEG NPs based combinational therapy holds promising potential for the treatment of breast cancer.

Keywords: Breast cancer- combination therapy- artimicinin- chrysin-hTERT

Introduction

Cancer is one of the most problematic health issues world wild (Jafari-Gharabaghlou et al., 2018; Javan et al., 2019). Breast cancer is the second rates in incidence and mortality in both sexes. Breast cancer is a serious global health concern for women in developed and developing nations. Breast cancer has several subtypes (Dadashpour et al., 2022).

Due to the heterogeneity of breast cancer, it is difficult to treat breast cancer in some patients with conventional therapies such as radiation therapy, chemotherapy, surgery, immunotherapy, and hormone therapy (Chatran et al., 2018). Despite new methods of treatments and chemotherapy medicine, concerns such as relapse, a significant reduction in quality of life, and serious side effects resulted in this type of treatment cannot be ignored (Júnior et al., 2019). Therefore, the search for new compounds with anti-cancer potential is essential.

Phytochemicals are natural compounds derived from medicinal plants as secondary metabolites. They have various biological functions, including anti-inflammatory, anti-cancer effects and antioxidant effects (Russo et al., 2010; Zyad et al., 2018). According to numerous studies, phytochemicals are applied as chemo-preventive and chemotherapeutic compounds in various types of cancer (Abbasi et al., 2018). The use of phytochemicals in combination with other cytotoxic drugs can increase the anti-cancer effect and reduce the side effects on normal cells and also combined treatment can delay resistance onset (SH Darvish Alipour, 2012).

Chr is a natural flavonoid that found in some

[1]Department of Genetics, Tehran Medical Sciences Branch, Islamic Azad University, Tehran, Iran. [2]Department of Biotechnology, Faculty of Medicine, Semnan University of Medical Sciences, Semnan, Iran. [3]Biotechnology Research Center, Semnan University of Medical Sciences, Semnan, Iran. [4]Department of Medicine, Faculty of Medicine, Istanbul Aydin University, Istanbul, Turkey. [5]Department of Clinical Biochemistry and Laboratory Medicine, Faculty of Medicine, Tabriz University of Medical Sciences, Tabriz, Iran. *For Correspondence: dadashpourm@semums.ac.ir, zarghamin@gmail.com

plants, especially chamomile, Pleurotus ostreatus, and honeycomb. Among the biological properties, the anti-cancer effects of Chr are significant (Mohammadian et al., 2016). Chr exerts its anti-cancer effects by blocking and inhibiting cancer cells in a variety of ways, including apoptosis, autophagy, angiogenesis, and cell proliferation (Khoo et al., 2010). The potential effects of apoptosis on various cancer cells, including breast, prostate, thyroid, pancreas, NSCLC, and intestine, have been documented (Sulaiman et al., 2018).

Art is derived form of the Chinese plant Artemisia annua. Art is registered as the standard protocol for the treatment of malaria based on its anti-malaria effects (Efferth, 2017). Beyond its anti-malarial effects, Art has shown anti-cancer and significant cytotoxic effects against a wide range of cancer types (Wong et al., 2017). The biological effects of Art and its derivatives in cancerous cells are inhibition of cancerous cells growth through cell cycle arrest, apoptosis, inhibition of angiogenesis, perturbation of angiogenesis and nuclear receptor responsiveness (Wong et al., 2017). Its anti-cancer properties in various cancer cells including breast, prostate, ovary, cervix, leukemia cells in in vivo and in vitro states have been studied and recorded (Zyad et al., 2018).

Nanotechnology is a technology in nanometer dimensions whose functional properties originate more than its size (Nejati et al., 2021b). Art and Chr have some disadvantages and limitations that reduce their biological function, but these limitations are significantly compensated by the advances in nanotechnology. These limitations include short half-life, low solubility, poor biological availability, low duration of stability in the bloodstream, and rapid metabolism and degradation. One of the most successful polymer nanoparticles is PLGA. It is a degradable polymer nanoparticle approved by the FDA and EMA due to its conversion into natural monomeric metabolites of glycolic acid and lactic acid in the body (Serati-Nouri et al., 2020; Mousazadeh et al., 2021). Therefore, encapsulation of anti-cancer phytochemicals such as Art and Chr in PLGA-PEG biodegradable nanoparticles may have many advantages over other drug delivery systems.

Studies show that more than 90% of cancer cells have changes in telomerase gene expression (Mogheri et al., 2021). The *hTERC* gene is expressed in normal and cancerous cells either, but the *hTERT* gene is expressed only in stem cells and cancer cells after embryonic development. Due to the high expressed *hTERT* gene in cancerous cells, targeting and inhibiting the expression of the *hTERT* gene in the cancer treatment is an acceptable idea for researchers (Singh and Khangotra, 2019; De Vitis et al., 2018). Knowing the exact mechanisms and pathways in the growth of breast cancer allows us to have a better targeted and more effective pathway in the treatment of breast cancer incorporating new technologies (Sawyers, 2004; Gasparini et al., 2005). In this study, the anti-cancer effects of Art and Chr on expressed *hTERT* gene in the T47D cell line of breast cancer cells were investigated in pure form and nanoencapsulated form, both individually and in combination.

Materials and Methods

Material

Fetal bovine serum (FBS) and RPMI 1640 were purchased from Gibco. Penicillin G, streptomycin, DMSO (Dimethylsulfoxide), MTT (3-(4, 5-Dimethylthiazol-2-yl)-2, 5-Diphenyltetrazolium Bromide), DL-Lactide, glycolide, polyethylene glycol (PEG, molecular weight: 4000), stannous octoate [Sn(Oct)2], alcoholic polyvinyl(PVA), dichloromethane (DCM), Art and Chr were purchased from Sigma-Aldrich. RPMI 1640, Streptomycin, penicillin G and fetal bovine serum (FBS) were obtained from Gibco. Sodium bicarbonate was purchased from Merk. Termo Fisher. RiboEx (total RNA isolation solution) from Gene All`s company has sold the first strand of cDNA synthesis kit and SYBER Green PCR Master Mix.

Cell culture and cell line

T47D human breast cell line cultured in RPMI 1640 complemented with 0.08 mg/ml streptomycin, 0.05 mg/ml penicillin G, 2 mg/ml sodium bicarbonate, 10% heat-inactivated fetal bovine serum (FBS), and were grown at 37°C in an incubator with 55% humidity and 5% CO_2.

Synthesis of PLGA-PEG

Preparation of PLGA-PEG was done through open ringed polymerization of glycolide and DL-lactide followed by PEG additional vacuum. PEG4000 and PLGA were copolymerized in presence of Sn(Oct)2 as the catalyst in polymerized melt mentioned before. Melting process was done through glycolide (0.570g), DL-lactide (2.882 g) and PEG4000 (1.54 g) bottleneck flask at 140°C under a nitrogen atmosphere. Mixture reaction comprising a 1:3 proportion of glycolide to DL-lactide and 0.05% (W/W) stannous octoate was made, heated to 175°C and kept for 4 hours (Santoveña et al., 2017).

Preparation of nanoparticles containing drug

Generally, encapsulation in PLGA-PEG nanoparticle of drugs was occurred via double emulsion (W/O/W) method with a minor modification. In brief, 20 mg of Chr and 200 mg of PLGA-PEG were dissolved in DCM and sonicated for 1 minute to allow Chr to be entrapped within the nanoparticle network (the W/O primary mixture). PVL and DMSO 1% (1:1) were added to W/O emulsion then sonicated for 1 minute to produce W/O/W emulsion. Then, DCM was evaporated using a rotary evaporator and the remaining solution was centrifuged at 10,000 rpm for 30 minutes.

Characterization of the nanoparticles containing drug

FT-IR, SEM and DLS methods have been utilized to study and analyze the physicochemical properties of drug-containing nanoparticles. Using FT-IR spectroscopy, various vibrations of functional groups in the structure of the prepared branched polymers (drug-loaded nanoparticles) such as carbonyl, ether, methylene and other groups have been investigated. Separately, a certain concentration (0.5%) of PLGA-PEG, Art NPs, Chr NPs

and Art/Chr NPS copolymers were prepared in KBr disks.

Using scanning electron microscope (SEM), morphology and surface topology of nanoparticles were studied. The size and morphology of the lyophilized sample of Art/Chr NPs were imaged under vacuum pressure, using a below 30 kW voltage and with various magnifications. Before performing SEM imaging, the sample was coated with a thin layer of gold metal (about a few angstroms).

Analyzing and determining particles size in range of few nanometers, microns or even smaller than nano have been possible by using dynamic light scattering (DLS) which is a physical method. The method mentioned is dependent on interaction of light and particle. Scattered light by nanoparticles in suspension (liquid medium) changes during a period of time that could be related to the particle diameter.

In vitro evaluation drug release

Drug release from the PLGA-PEG NPs was determined using dialysis. Briefly, 25 mg Art/Chr PLGA-PEG NPs, dissolved in 5 mL PBS and transferred to a dialysis membrane tube (MW cut off 3000) and placed in 30 mL PBS which was shaken with a stirrer at 120 rpm at the temperature of 37°C. For 160 hours, the PBS medium was repeatedly replaced at regular intervals, and the studied compounds (Chr NPs, Art NPs and Art/Chr NPs) were taken in the previous medium at a wavelength of 348 nm for Chr, 203 nm for Art (maximum wavelength).

Cell viability and MTT-based cytotoxicity assay

Effect of Art, Chr and Art/Chr cytotoxicity in pure and in nanoencapsulated form on the T47D cell line using MTT assay was studied in 48-hour. MTT is a water-soluble yellow substance that is regenerated in living cells as a result of the action of the enzyme succinate dehydrogenase and turns into a purple substance called formazan, which is insoluble in the aqueous phase.

In brief, T47D cell line were cultured in an incubator at 37°C in a humid atmosphere containing 5% CO_2, which is required to strengthen cell binding. After cell culture and passage, the number of cells has reached a sufficient amount and subsequently 3,000 cells were seeded in 96-well plates. In the incubator, the cells were given 24 hours to adhere to the wells. After 48 hours, 4 series of dilutions from each of Art, Chr, Art/Chr, Art NPs, Chr NPs and Art/Chr NPs were prepared from the drug stock and were treated in triplicates in the wells. After 48 hours of incubation, IC_{50} was assessed by MTT assay. For this purpose, the culture medium inside the wells was gently removed and 200 µl MTT solution (for every 1 mL of PBS, 2 mg of MTT powder) was poured into each well and the plates were covered with aluminum foil and incubated for 4 hours at 37°C. After 4 hours, the surface of the wells was gently removed, and the formed insoluble purple crystals of Formazan were dissolved by adding 200 µl DMSO to each well by placing it on an orbital shaker for 10 minutes (at this stage the plates are still covered with aluminum foil). In the next step, the absorption rate of each well was read and recorded at 570 nm using an EL X 800 microplate absorbance reader (Bio Tek Instruments,

Winooski, VT) with a reference wavelength of 630 nm.

Quantitative real-time PCR assay

Real-time PCR was used to evaluate the changes in *hTERT* gene expression in the T47D cell line after drug treatment. For real-time PCR, RNA total was extracted, then cDNA synthesis, and then RT-PCR. For this purpose, 300,000 cells were cultured in 6-well plates. The cells were treated using 6 studied compounds (drug dilution less than IC_{50}) for 24 hours and one well was grown as a control measure with culture medium only. Then the RNA total of each well was extracted using the effective and fast method of Trizol reagent (Ribo Ex total RNA-Gene All) considering to the manufacturer's instructions. During the extraction process, isopropanol causes RNA deposition. To analyze the RNA total quantity, a nanodrop device was used, and the OD260 / OD280 calculation showed the purity of the extracted RNA total. To analyze RNA total quality 1% agarose gel electrophoresis was used. Next, first Strand cDNA synthesis kit made by Thermo Fisher Scientific Company was used for cDNA synthesis.

In this study, the analysis of RT-PCR data is a relative evaluation method. This is a more accurate method to examine changes in gene expression. In this method, the studied gene (hTERT) is compared with a reference gene as an internal control which in this study is considered β–actin. For RT-PCR, primers related to the *hTERT* gene were designed by Primer3 software and synthesized by Takpajohan Gene Company.

Statistical analysis

All experiments were carried out in triplicate and data were represented as mean values ± standard error (SE) of the experiments. GraphPad 6 Prism software (CA, USA) was employed to evaluate statistical significance between study groups using T-test for comparison between two groups and one-way analysis of variance for comparison between more than two groups. P values less than 0.05 were regarded statistically significant.

Results

Characterization of drug-loaded PLGA/PEG NPs
FT-IR spectroscopy

FT-IR spectroscopy was utilized to confirm the encapsulation of Art and Chr in PLGA-PEG (Figure 1). In the IR spectrum related to PLGA-PEG copolymer, absorption band 3,454.52 cm^{-1} belongs to hydroxyl groups, absorption band 3,130.20 cm^{-1} corresponds to COOH, absorption band 1,637.04 cm^{-1} correlates with the tensile vibrations of the C = O group (related to ester), absorption bands in the range of 1,082.21 cm^{-1} belong to the tensile vibrations of the C-O-C bond (related to PEG), and absorption bands in the range of 1,188.19 cm^{-1} corresponds to C-O. The infrared spectroscopy of pure Artemisinin, absorption bands 2913.14 cm^{-1} and 3,453.06 cm^{-1} correlates with N-H vibrations, absorption band 1,739.64 cm^{-1} belongs to the tensile vibrations of C-O, and range of 1,380.96 cm^{-1} to 1,457.38 cm^{-1} corresponds to C-H. Displayed in, the infrared spectroscopy of Chr, absorption band 2,884.78 cm^{-1} belongs to the vibrations of the C-H

Leila Khoshravan Azar et al

Table 1. Characterization of PLGA-PEG and Drug-Loaded PLGA-PEG NPs. Results are expressed as mean ± SD of three different measurements (n=3).

Groups	Particle size (nm)*	Polydispersity	Zeta potential (mV)*
PLGA-PEG NPs	80±2.17	0.133	−25.2±2.4
Chr loaded PLGA-PEG NPs	90±3.40	0.169	−28.4±2.7
Art loaded PLGA-PEG NPs	95±3.57	0.17	−18.7±1.0
Chr/Art loaded PLGA-PEG NPs	110±7.12	0.224	−15.6±1.3

Figure 1. FTIR Spectra of Art/Chr -Loaded PLGA-PEG NPs (A), Art (B), Chr (C) and PLGA-PEG (D).

group, absorption band 1,653.07 cm^{-1} corresponds to the tensile vibrations of the carbonyl group C-O, and absorption bands of 906.42 cm^{-1} to 1,027.48 cm^{-1} correlate with the C-C, C-O, and C-O-C bonds. The IR spectrum of PLGA-PEG copolymer containing Art/Chr, absorption band in range of 1,737.53 cm^{-1} belongs to the hydroxyl groups, absorption band 2,916.68 cm^{-1} corresponds to the vibrations of N-H, absorption band 1,737.53 cm^{-1} correlates with the C-O bond, absorption band 1,453.47 cm^{-1} belongs to the C-H bond, absorption band 1,094.44 cm^{-1} corresponds to C-O-C bond. The matching of the absorption bands in Art/Chr NPs with the pure Artemisinin and pure Chrysin absorption bands indicates that both drugs are encapsulated in nanoparticles (PLGA-PEG).
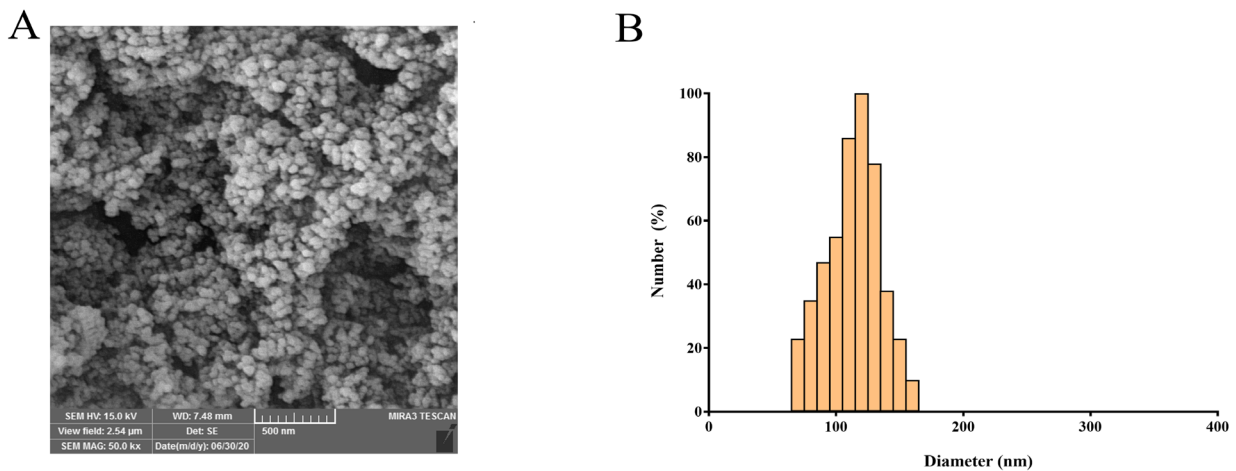

Figure 2. Characterization of Art/Chr -loaded PLGA-PEG NPs. Field emission scanning electron microscopy (FE-SEM) (A). Dynamic light scattering (DLS)(B).
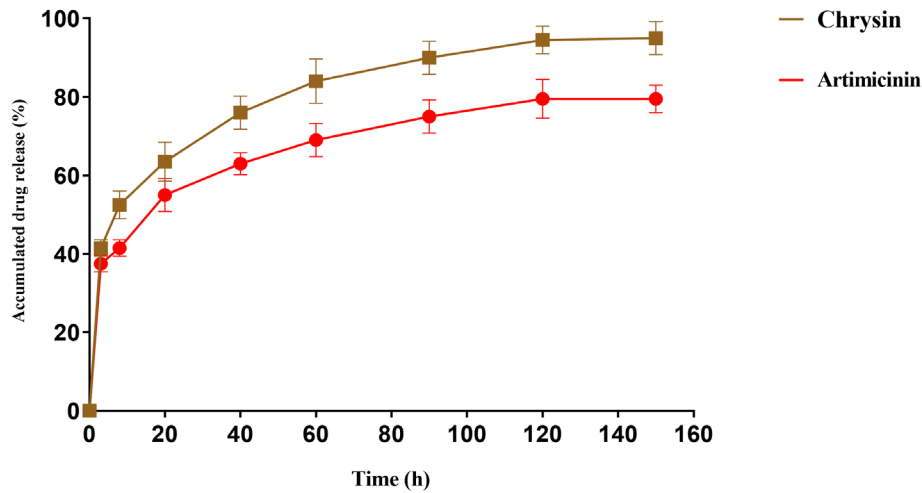
Figure 3. Drug Release Profiles of Art and Chr from PLGA-PEG NPs in PBS at pH 7.4. Results are presented as mean ± SD (n=3).

Table 2. IC$_{50}$ Values for T47D Cell Line Treated with Pure and Nanofurmolated of Each Drug within 48h.

Incubation time (h)	IC$_{50}$ values (μM) Mean ± SD					
	Chr	Chr loaded PLGA-PEG	Art	Art loaded PLGA-PEG	Art/Chr	Art/Chr loaded PLGA-PEG
24 h	25.73	18.61	21.36	17.15	18.12	12.51

Surface morphology

The spherical shapes and uniform distributions of PLGA-PEG and Art/Chr PLGA-PEG NPs were further confirmed using FE-SEM image. From these micrographs, the PLGA-PEG NPs showed a spherical uniformed shape and their dimensions varied between 20 and 65 nm (Figure 2A). After encapsulating and formatting of Art/Chr-PLGA-PEG NPs, the size of particle changed to about 120 nm.

Investigation of the size distribution

The mean diameter/size distribution profile, PDI, and zeta potential of Chr/ Art NPs were by DLS. Nanoparticle dimension analysis via DLS shows a median dimension of 110 nm with uniform dispersion for PLGA-PEG nanoparticles. It was also observed that Art NPs and Chr NPs have an average dimension of 70 nm with a range between 70 and 120 and Art/Chr NPs have an average size of 110 nm with a range between about 80 to 180. (Figure 2B). The characterization of PLGA-PEG-loaded drugs are reported in Table 2.

Entrapment Efficiency (EE) and drug loading (DL)

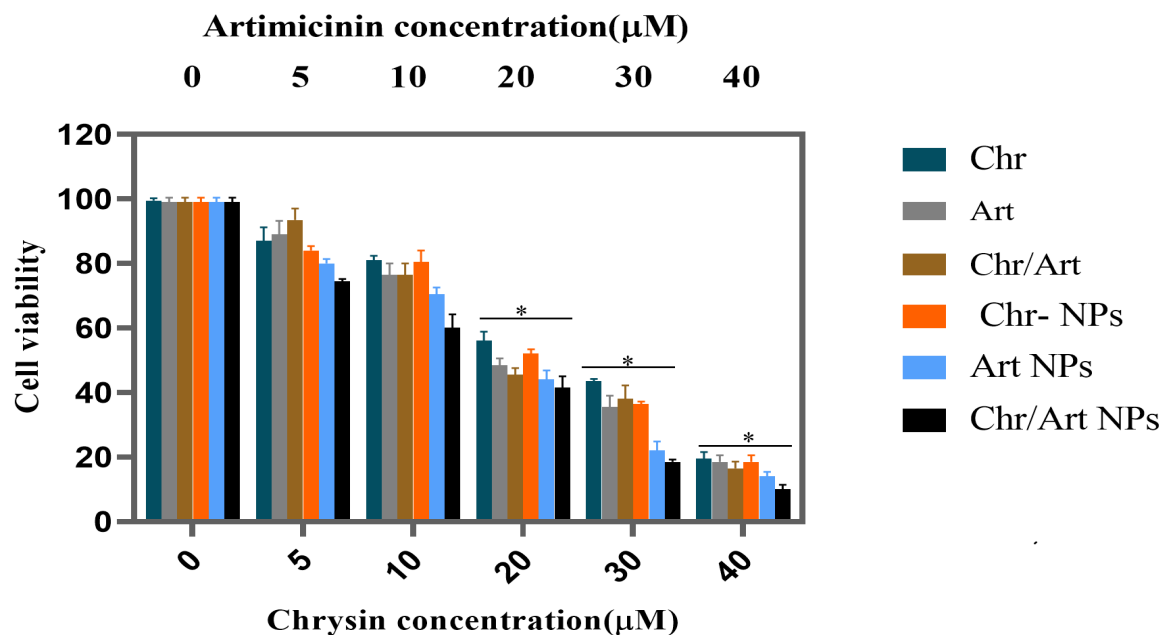The nanoencapsulation efficiency of Chr, Art and Art/

Figure 4. *In vitro* Cytotoxicity of Art, Chr, Art/Chr, Art NPs, Chr NPs and Art/Chr NPs against T47D cells at 24h.
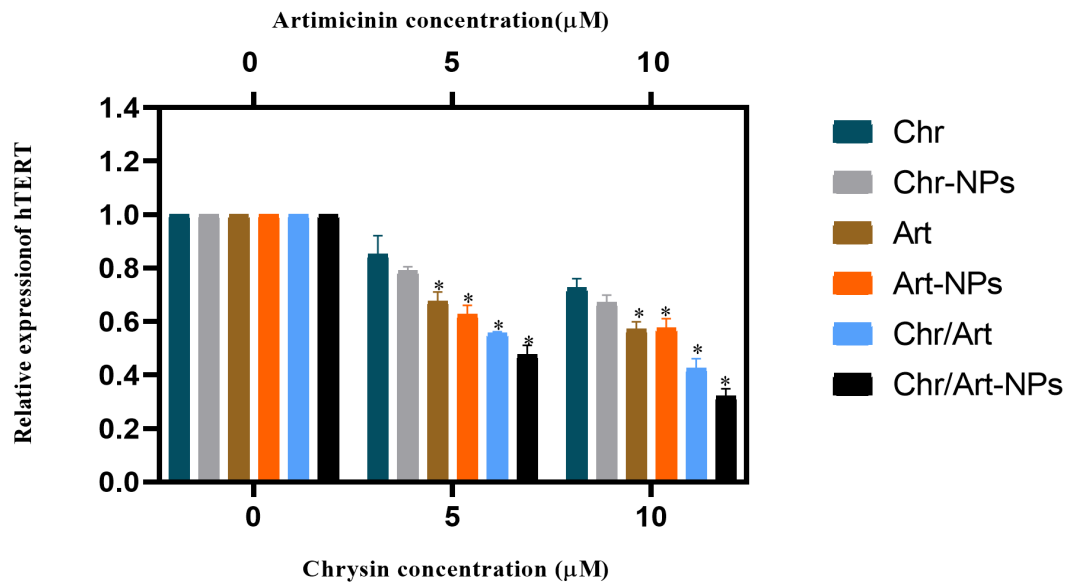
Figure 5. The Expression Levels of *hTERT* Genes Relative to Reference Gene (GAPDH) in T47D Cells Treated with Art, Chr, Art/Chr, Art NPs, Chr NPs and Art/Chr NPs.

Chr were found to be $85.3 \pm 2.6\%$, 78.16% and 79.27%, respectively. Moreover, the capacity of drug loading of Art and Chr found to be $14.8 \pm 1.3\%$ and $14.1 \pm 5.1\%$, respectively. It seems that the high encapsulation efficacy of these natural antitumor drugs is due to their hydrophobic nature

Release rate Art and Chr from PLGA-PEG NPs

The kinetics of Art and Chr drugs loaded in 160 hours were examined in in vitro state (Figure 3). The amount of Art and Chr released in the first 20 hours was almost equal, subsequently, the release of both drugs was increasing, but the amount of Chr released was much higher compared to Art. After the first 120 hours of the rest of the phase, the rate of Chr release was noticeably higher than of Art. Overall, however, both drugs showed a significant increase in release within 160 hours.

In vitro cytotoxicity study

MTT assay is an essential technique of assessing the biological materials` cytotoxicity in in vitro state. In this study, the results of cytotoxicity assay for the treatment of T47D cells with different concentrations of pure and nanoencapsulated Art, pure and nanoencapsulated Chr, pure and nanoencapsulated Art/Chr; Shown in Figures 4 at 48 hours. The results obtained from the graphs show that all 6 compounds have got an inhibitory effect on the T47D cell line. It can also be seen from the graphs that each of the drugs in the nano state has a greater degree of inhibition than in their pure state. Among the all samples, Art/Chr NPs had the greatest inhibitory effect at all concentrations treated at 48 hours. After Art/Chr NPs, Art NPs have shown the greatest inhibitory effect on all concentrations in both periods. Also, Table 3 shows the mean IC_{50} values (Mean $\pm$ SD) for the T47D cell line of breast cancer after treatment with 6 studied compounds during 48 hours. The IC_{50} results indicate the inhibitory performance of all 6

compounds, especially nanoencapsulated compounds, and show the highest performance among nanocapsules, Art/Chr NPs.

Real-time PCR and RNA total extraction results

A real-time PCR technique was applied to quantify expression of the *hTERT* gene in T47D cells treated with concentrations of 5 and 10 μM of Art, Chr and Art/Chr, in both pure and nanoencapsulated form after 24 h of incubation. By increasing the concentration of Art, Chr and Art/Chr in pure and nanocapsules, because of the high effect of these compounds on reducing the expression of *hTERT* gene in treated samples and high concentrations of drug in real-time PCR due to lower mRNA expression, T47D treatment reach the threshold of Ct in the above cycles. Therefore, high concentrations have not been tested for this study. As Figure 5 shows, all 6 drugs showed a remarkable reduction in hTERT expression of T47D breast cancer. Nanoencapsulated drugs have a greater inhibitory effect on *hTERT* gene expression than the pure state. The results also show a greater inhibitory effect of combination drugs in both pure and nanoencapsulated states. The difference was statistically significant ($p \leq 0.05$).

Discussion

It is reported that global statistics on female breast cancer is one of the most common cancer. Despite the increase in survival rate and decrease in mortality rate, the side effects and negative impact on life quality of most patients during treatment cannot be ignored (Adlravan et al., 2021). Therefore, for preventing and treatment of breast cancer, a more optimal method of treatment without these side effects is a vital action (Nejati et al., 2021a) . Due to their low toxicity and a wide range of biological activities, phytochemicals can be utilized as an alternative method of treatment. The anticancer effects of the

phytochemical Art have been proven in numerous studies. It exerts its anti-cancer properties in various ways (Wong et al., 2017). The level of iron are remarkably higher in cancerous cells than normal cells, and iron breaks down the endoperoxide structure in Art, leading to cell death (Li et al., 2021). Studies conducted by Guo-Qing Chen et al. in 2019 demonstrated Art's antitumor property by direction breast TNCB cancer cells to ferroptosis, which is a type of cell death (Chen et al., 2020). Also in studies conducted on normal and cancerous breast cell lines in 24 hours of treatment with Art has shown that it has a cytotoxic and inhibitory effect by reducing proliferation, migration, invasion, and apoptosis on MCF-7, T47D, and MDA-MB-231 and had no effect on normal MCF-10A cells. The biological and anti-cancer properties of the phytochemical Chr have been revealed by researchers and are therefore used in treating of many diseases including cancer. One study showed that Chr NPs and modified Chr NPs (PLGA-PVA) display the inhibitory effect on the MCF-7 breast cancer cell line and SKOV-3 ovarian cancer cell line (Sulaiman et al., 2018). Using multiple drugs for the same purpose and the same cellular pathways can have an essential and functional role in effectiveness of more and better complete treatment. Several studies have been conducted on the effectiveness of Art in combination cancer therapies. The synergistic effect of Art medication in combination with other compounds to increase the therapeutic effect and reduce the side effects of cancer therapies has been documented in cell lines and animal testing. According to research, the anti-cancer effect of Art is significantly increased when used with flavonoids. Though, in combination therapies, Art has not always shown a synergistic effect (Ferreira et al., 2010; Efferth, 2017). Another study displayed the synergistic effect of Art with a wide range of drugs, including some flavonoid compounds. It can even be used to increase the therapeutic effect of radiotherapy and other macromolecules such as recombinant protein and therapeutic nucleic acid (Efferth, 2017). In this study, Art and Chr showed a synergistic effect in drug combination form, so that Art/Chr had lower IC_{50} than Art and Chr separately with similar concentrations, which indicates the greater cytotoxic effect of the drug combination. Nanotechnology-based approaches offer significant potential for addressing therapeutic vulnerabilities, including cancer. Therefore, in several studies using nanoencapsulation, the limitations of phytochemicals are significantly compensated, and their biological potential is increased (Jain et al., 2020). In research, nanoencapsulated phytochemicals have far greater antitumor effects than in pure form. In one study, the effect of metformin nanocapsules showed a greater inhibitory effect than pure metformin by reducing the expression of the *hTERT* gene in T47D and MDA-MB-231 cell lines in in vitro. In another study, the effect of Curcumin and Chrysin in the nanoencapsulated form in the SW480 cell line of colorectal cancer was more than their pure form (Javidfar et al., 2018). In the present study, Art NPs, Chr NPs and Art/Chr NPs at concentrations of 20, 30 and 40 μM at 48 hours had a greater cytotoxic effect compared to pure form.

Much more effective treatment methods have been created by the new molecular target therapy (Gasparini et al., 2005). Alterations in telomerase gene expression are one of the most essential and key factors in cancer cells. In this regard, several studies have been performed on the inhibition of cancer cells by reducing telomerase activity (Ganesan and Xu, 2018). In these studies, Sil-PLGA/PEG at different concentrations reduced expression of the *hTERT* gene in the T47D cell line had an inhibitory effect on breast cancer cells. With studies on the level of telomerase gene expression, researchers believe that future research centers will focus on regulating telomerase gene expression to present a new strategy for cancer treatment (Leão et al., 2018; Guterres and Villanueva, 2020). In confirmation of previous research, in this study, the T47D cell line of breast cancer was inhibited by reducing the expression of the *hTERT* gene and telomerase activity.

In conclusion, in this present study, Art and Chr-loaded PLGA-PEG NPs were successfully prepared using the w/o/w method in the presence of PVA as a stabilizer. Morphological and particle size analysis displayed that the synthesized Art and Chr -loaded PLGA-PEG NPs displayed approximate spherical shapes with smooth surfaces and an average particle size <110 nm. Based on our results, combinational nanoformulated of Art–Chr was be capable of killing T47D cancer cells more greater than either treatment alone, thereby potentially this strategy can reduce cytotoxicity and patient side effects. Moreover, the co-delivery of Art and Chr by PLGA/PEG nanocarrier suppresses hTERT expression more efficiently in relative to the delivery of either Art or Chr at the same concentrations, indicating a synergistic manner. These results suggest that the nano-encapsulation of Art and Chr in PLGA-PEG copolymers can provide an attractive drug delivery approach for the treatment of breast cancer. Further in vivo examination should be conducted to clarify the therapeutic efficacy of these Art/Chr-loaded PLGA-PEG NPs.

Author Contribution Statement

Leila Khoshravan: Methodology, Investigation, Data curation, Original draft preparation. Mehdi Dadashpour and Mehrdad Hashemi: Writing- Reviewing and Editing. Nosratollah Zarghami: Supervision, Conceptualization, funding acquisition, Reviewing and Editing.

Acknowledgements

Availability of data and materials
The analyzed data during the current study are available from the corresponding authors on reasonable request

Ethics approval and consent to participate
The Ethics Committee of Faculty of Pharmacy

and Pharmaceutical Sciences- Tehran Islamic Azad University of Medical Sciences, Tehran has approved the current study and written informed consent was obtained from all of the participants (Code of Ethics: IR.IAU. PS.REC.1399.166).

Declaration of interest

The authors' statement has no conflicts of interest in this article content.

References

Abbasi BA, Iqbal J, Mahmood T, et al (2018). Role of dietary phytochemicals in modulation of miRNA expression: Natural swords combating breast cancer. *Asian Pac J Trop Med*, **11**, 501.

Adlravan E, Nejati K, Karimi MA, et al (2021). Potential activity of free and PLGA/PEG nanoencapsulated nasturtium officinale extract in inducing cytotoxicity and apoptosis in human lung carcinoma A549 cells. *J Drug Deliv Sci Technol*, **61**, 102256.

Chatran M, Pilehvar-Soltanahmadi Y, Dadashpour M, et al (2018). Synergistic anti-proliferative effects of metformin and silibinin combination on T47D breast cancer cells via hTERT and cyclin D1 inhibition. *Drug Res*, **68**, 710-6.

Chen G-Q, Benthani FA, Wu J, et al (2020). Artemisinin compounds sensitize cancer cells to ferroptosis by regulating iron homeostasis. *Cell Death Different*, **27**, 242-54.

Dadashpour M, Ganjibakhsh M, Mousazadeh H, et al (2022). Increased pro-apoptotic and anti-proliferative activities of simvastatin encapsulated PCL-PEG nanoparticles on human breast cancer adenocarcinoma cells. *J Cluster Sci*, **2022**, 1-12.

De Vitis M, Berardinelli F, Sgura A (2018). Telomere length maintenance in cancer: at the crossroad between telomerase and alternative lengthening of telomeres (ALT). *Int J Mol Sci*, **19**, 606.

Efferth T (2017). Cancer combination therapies with artemisinin-type drugs. *Biochem Pharmacol*, **139**, 56-70.

Ferreira JF, Luthria DL, Sasaki T, et al (2010). Flavonoids from Artemisia annua L. as antioxidants and their potential synergism with artemisinin against malaria and cancer. *Molecules*, **15**, 3135-70.

Ganesan K, Xu B (2018). Telomerase inhibitors from natural products and their anticancer potential. *Int J Mol Sci*, **19**, 13.

Gasparini G, Longo R, Torino F, et al (2005). Therapy of breast cancer with molecular targeting agents. *Ann Oncol*, **16**, iv28-iv36.

Guterres AN, Villanueva J (2020). Targeting telomerase for cancer therapy. *Oncogene*, **39**, 5811-24.

Jafari-Gharabaghlou D, Pilehvar-Soltanahmadi Y, Dadashpour M, et al (2018). Combination of metformin and phenformin synergistically inhibits proliferation and hTERT expression in human breast cancer cells. *Iran J Basic Med Sci*, **21**, 1167.

Javan ES, Lotfi F, Jafari-Gharabaghlou D, Mousazadeh H, et al (2022). Development of a magnetic nanostructure for co-delivery of metformin and silibinin on growth of lung cancer cells: Possible Action Through Leptin Gene and its Receptor Regulation. *Asian Pac J Cancer Prev*, **23**, 519-27.

Jain V, Kumar H, Anod HV, et al (2020). A review of nanotechnology-based approaches for breast cancer and triple-negative breast cancer. *J Controlled Release*, **2020**.

Javan N, Khadem Ansari MH, Dadashpour M, et al (2019). Synergistic antiproliferative effects of co-nanoencapsulated curcumin and chrysin on mda-mb-231 breast cancer cells through upregulating mir-132 and mir-502c. *Nutr Cancer*, **71**, 1201-13.

Javidfar S, Pilehvar-Soltanahmadi Y, Farajzadeh R, et al (2018). The inhibitory effects of nano-encapsulated metformin on growth and hTERT expression in breast cancer cells. *J Drug Deliv Sci Technol*, **43**, 19-26.

Júnior RGO, Ferraz CAA, Pereira ECV, et al (2019). Phytochemical analysis and cytotoxic activity of Cnidoscolus quercifolius Pohl (Euphorbiaceae) against prostate (PC3 and PC3-M) and breast (MCF-7) cancer cells. *Pharmacognosy Magazine*, **15**, 24.

Khoo BY, Chua SL, Balaram P (2010). Apoptotic effects of chrysin in human cancer cell lines. *Int J Mol Sci*, **11**, 2188-99.

Leão R, Apolónio JD, Lee D, et al (2018). Mechanisms of human telomerase reverse transcriptase (h TERT) regulation: clinical impacts in cancer. *J Biomed Sci*, **25**, 1-12.

Li Z, Wu X, Wang W, et al (2021). Fe (II) and Tannic Acid-Cloaked MOF as carrier of artemisinin for supply of Ferrous Ions to enhance treatment of triple-negative breast cancer. *Nanoscale Res Lett*, **16**, 1-11.

Maasomi ZJ, Soltanahmadi YP, Dadashpour M, et al (2017). Synergistic anticancer effects of silibinin and chrysin in T47D breast cancer cells. *Asian Pac J Cancer Prev*, **18**, 1283.

Mogheri F, Jokar E, Afshin R, et al (2021). Co-delivery of metformin and silibinin in dual-drug loaded nanoparticles synergistically improves chemotherapy in human non-small cell lung cancer A549 cells. *J Drug Deliv Sci Technol*, **66**, 102752.

Mohammadian F, Abhari A, Dariushnejad H, et al (2016). Effects of chrysin-PLGA-PEG nanoparticles on proliferation and gene expression of miRNAs in gastric cancer cell line. *Iran J Cancer Prev*, **9**.

Mousazadeh H, Pilehvar-Soltanahmadi Y, Dadashpour M, et al (2021). Cyclodextrin based natural nanostructured carbohydrate polymers as effective non-viral siRNA delivery systems for cancer gene therapy. *J Controlled Release*, **330**, 1046-70.

Nejati K, Alivand M, Arabzadeh A (2021a). MicroRNA-22 in female malignancies: focusing on breast, cervical, and ovarian cancers. *Pathol Res Pract*, **2021**, 153452.

Nejati K, Dadashpour M, Gharibi T, et al (2021b). Biomedical applications of functionalized gold nanoparticles: A Review. *J Cluster Sci*, **2021**, 1-16.

Russo M, Spagnuolo C, Tedesco I, et al (2010). Phytochemicals in cancer prevention and therapy: truth or dare?. *Toxins*, **2**, 517-51.

Santoveña A, Monzón C, Alvarez-Lorenzo C, et al (2017). Structure-performance relationships of temperature-responsive PLGA-PEG-PLGA gels for sustained release of bone morphogenetic protein-2. *J Pharm Sci*, **106**, 3353-62.

Sawyers C (2004). Targeted cancer therapy. *Nature*, **432**, 294-7.

Serati-Nouri H, Jafari A, Roshangar L, et al (2020). Biomedical applications of zeolite-based materials: A review. *Materials Sci Engin C*, **116**, 111225.

SH Darvish Alipour A (2012). Comparison of ferrous ion chelating, free radical scavenging and anti tyrosinase properties of Thymus daenensis essential oil with commercial thyme oil and thymol. *J Adv Med Biomed Res*, **19**, 77.

Singh Z, Khangotra P (2019). Human telomerase reverse transcriptase as a major therapeutic target in different cancer types. *Trends Med*, **19**, 1-4.

Sulaiman GM, Jabir MS, Hameed AH (2018). Nanoscale modification of chrysin for improved of therapeutic efficiency and cytotoxicity. *Artif Cells Nanomed Biotechnol*, **46**, 708-20.

Wong YK, Xu C, Kalesh KA, et al (2017). Artemisinin as an anticancer drug: recent advances in target profiling and mechanisms of action. *Med Res Rev*, **37**, 1492-517.

Zyad A, Tilaoui M, Jaafari A, et al (2018). More insights into the pharmacological effects of artemisinin. *Phytother Res*, **32**, 216-29.